

# An inventory and population-scale analysis of martian glacier-like forms

Colin Souness<sup>a,\*</sup>, Bryn Hubbard<sup>a</sup>, Ralph E. Milliken<sup>b</sup>, Duncan Quincey<sup>a</sup>

<sup>a</sup> Institute of Geography and Earth Sciences, Aberystwyth University, Aberystwyth, UK

<sup>b</sup> Dept. Civil Engineering and Geological Sciences, University of Notre Dame, Notre Dame, IN 46556, USA

## ARTICLE INFO

### Article history:

Received 7 June 2011

Revised 29 September 2011

Accepted 24 October 2011

Available online 3 November 2011

### Keywords:

Ices  
Mars  
Mars, Surface  
Mars, Climate  
Mars, Polar caps

## ABSTRACT

Martian glacier-like forms (GLFs) indicate that water ice has undergone deformation on the planet within its recent geological past, but the driving mechanisms behind the origin, evolution and dynamics of these landforms remain poorly understood. Here, we present the results of a comprehensive inventory of GLFs, derived from a database of 8058 Context Camera (CTX) images, to describe the physical controls on GLF concentration and morphometry. The inventory identifies 1309 GLFs (727 GLFs in the northern hemisphere and 582 in the southern hemisphere) clustered in the mid-latitudes (centred on a mean latitude of 39.3° in the north and −40.7° in the south) and in areas of rough topography. Morphometric data show inter-hemispheric similarity in GLF length (mean = 4.66 km) and width (mean = 1.27 km), suggesting a common evolutionary history, and a poleward orientation of GLFs in both hemispheres, indicating a sensitivity to climate and insolation. On a local scale, elevation is shown to be the most important control on GLF location, with most GLFs occurring above an altitude threshold of −3000 m (AOD), and in areas of moderate, but not high, relief. We propose, therefore, that martian GLFs may not exhibit accumulation or ablation areas as is the norm for terrestrial glacial systems, but reflect ice motion in response to local relief within a widely distributed reservoir of ice deposited within prescribed latitudinal and elevational ranges.

© 2011 Elsevier Inc. All rights reserved.

## 1. Introduction

In recent years, the acquisition of very high-resolution images of the martian surface has resulted in various aspects of Mars' landscape coming under increased scrutiny. The result of this is that our understanding of the geological processes which operate at and near the martian surface has become more fully developed. One suite of landforms that has received particular attention is that associated with the presence of, and processes relating to, water ice. Indeed, it is widely held that Mars' recent geological past has been dominated by the action of ice-rich processes (e.g. Kargel, 2004; Baker et al., 2010). Many of these landforms and landscape elements share visible characteristics with terrestrial glaciers (e.g. Marchant and Head, 2003; Head et al., 2005; Forget et al., 2006). The general appearance of these features strongly suggests down-slope flow and deformation, including indicators such as lobate structures, extensional troughs, compressional ridges, and, in many cases, elongated lateral and terminal ridges. Observations of such characteristics have led to the application of the term viscous flow feature or 'VFF' (Milliken et al., 2003). Milliken et al. (2003) defined VFFs as exhibiting: "primary or secondary lobate features of the material (typically in alcoves), lineations on the surface

(both parallel and transverse to the slope on which the material flows), compressional ridges or extensional troughs, ridges at the flow front or base of the slope, or other general evidence that the material flowed around or over obstacles such as craters or mounds".

Herein, we use 'VFF' as an umbrella term for all glacial-type formations exhibiting evidence of viscous flow. Although Milliken et al. (2003) referred to "metres-thick" deposits of ice, and work has subsequently been presented by other parties (e.g. Holt et al., 2008; Plaut et al., 2009) which suggests that some VFFs have mass depths greatly in excess of this, Milliken et al. (2003) included no requirement of depth in their identification criteria and the term 'viscous flow feature' itself makes no reference to depth, therefore we maintain it as being an appropriate descriptor in this context.

Squyres and Carr (1986) hypothesised that some large scale VFFs, commonly referred to as lobate debris aprons (LDAs), formed through the relaxation of topography underlain by an ice-saturated crust. Indeed, recent results from the Mars Reconnaissance Orbiter (MRO) shallow radar (SHARAD) instrument show that LDAs exhibit properties consistent with a dominantly water ice composition beneath a relatively thin dry surface (Holt et al., 2008; Plaut et al., 2009). Squyres and Carr (1986) also observed that VFFs occurred primarily between 30° and 60° in both hemispheres, with forms appearing to be notably less well-developed at latitudes above 55°. Later work supported these observations, and VFFs of various lengths have been described almost exclusively within Mars' mid-

\* Corresponding author.

E-mail address: [cjs07@aber.ac.uk](mailto:cjs07@aber.ac.uk) (C. Souness).

latitudes (Milliken et al., 2003; Head et al., 2010). Milliken et al. (2003) conducted a global survey of VFF distribution utilising 13,000 Mars Orbiter Camera (MOC) images. Of these images, 146 included one or more VFFs, almost all of which were located in the mid-latitudes, with the maximum frequency of occurrence lying on the 40° line of latitude in both hemispheres. This distribution is consistent with prevailing theories relating the origin of VFFs to Mars' climatic history which postulate that increased rotational obliquity as recently as  $\sim 5 \times 10^6$  years before present (Touma and Wisdom, 1993) permitted the equatorward migration of moisture from Mars' polar caps, allowing the accumulation (and subsequent flow) of water ice in Mars' mid-latitudes (Head et al., 2003; Forget et al., 2006; Schon et al., 2009). Climate modelling by Fanale et al. (1986) suggested that water ice from this past epoch could remain stable in the mid-latitudes under Mars' current climatic regime if shielded by dust or regolith. The findings of Holt et al. (2008) and Plaut et al. (2009) from SHARAD data have corroborated this hypothesis, raising the possibility that smaller scale VFFs may also contain water ice beneath a thin (0.5–10 m), 'dry' regolith layer.

The broadly-defined VFF suite of landforms (see above) includes many variations in morphology and apparent landscape association (e.g. Head et al., 2010). The morphologically distinctive sub-types of VFF include 'lineated valley fill' (LVF), broad and often extensive 'lobate debris aprons' (LDAs), and smaller alcove-fed 'glacier-like forms' (GLFs) (e.g. Li et al., 2005; Holt et al., 2008; Morgan et al., 2009; Plaut et al., 2009; Baker et al., 2010; Head et al., 2010; Hubbard et al., 2011) (Fig. 1). It should be noted that GLFs were originally termed 'glacier-like flows' by Arfstrom and Hartmann (2005). However, Hubbard et al. (2011) amended the term to 'glacier-like form' on the grounds that: (i) actual motion had not yet been measured, (ii) supplementary (basal) motion components had not yet been ruled out, and (iii) the term 'flow' can refer to either a feature or a process. Herein, we also use the term GLF to mean 'glacier-like form'.

Although the exact composition of icy deposits remains unconfirmed, all three sub-types of VFF (i.e. LVF, LDA and GLF) appear to be composed of a similar material and observations suggest the existence of close inter-relationships. For example, LVF is commonly interpreted to be the product of convergent LDAs, which themselves seem often to be fed by the lower-order alcove GLFs (Fig. 1a) (Head et al., 2010). GLFs in particular are visually and contextually very similar to terrestrial valley glaciers, having a broad,

topographically constrained upper basin that appears to feed material in a down-slope direction into a tongue that is often bordered by raised, moraine-like ridges (Arfstrom and Hartmann, 2005) (Fig. 1b and Fig. 2). Such moraine-like ridges may be the result of activity more recent than that responsible for the emplacement of higher-order LDAs and LVF (Baker et al., 2010). These and other similarities suggest that GLFs may be of particular value in explaining the origins and processes associated with all types of martian VFF, as it is these valley-glacier-like forms to which terrestrial glacial analogs can be most directly compared. However, direct comparisons with terrestrial analogs are somewhat complicated by the environmental differences between Earth and Mars (e.g. Pelletier et al., 2009).

At present neither the mass-balance relations nor the mechanisms by which VFFs flow are well understood. However, modelling by Milliken et al. (2003) showed that a  $\sim 10$  m thick layer of ice could produce the observed deformation landforms under present and past martian conditions within the time permitted by current age estimates ( $10^5$ – $10^7$  years), while an even thicker deposit would deform faster (Milliken et al., 2003).

On Earth, temperature and precipitation (along with the presence of a land base) exert the dominant controls on the global distribution of flowing glacier ice. These factors are in turn mediated by geographical variables including, most importantly, latitude and altitude. In a global context, ice accumulates at the lowest elevations towards the poles, where air temperatures are coldest. As ambient air temperatures increase towards the equator, the elevation at which permanent ice masses occur generally increases, with a superimposed precipitation effect (Sugden and John, 1990). This dependence on elevation initiates a regime of mass-balance and ice movement whereby ice accumulation above a threshold altitude (termed the equilibrium line altitude, or 'ELA') is broadly matched by annual flow through the ELA and ice loss below the ELA. This ELA is dynamic and its exact location varies to reflect changes in climate. The short-term ELA, for any given year, coincides with the position of the snowline visible on a glacier at the end of the melt season or dry season. The snow deposits remaining above the ELA represent mass accumulation; i.e. snow that has survived the melt season and will remain (after being buried beneath any snow that falls in the ensuing winter) into the next year. The overall shape of an ice mass is predominantly determined and subsequently maintained by the transfer of ice from this accumulation area into the ablation area. How this mass-balance regime operates

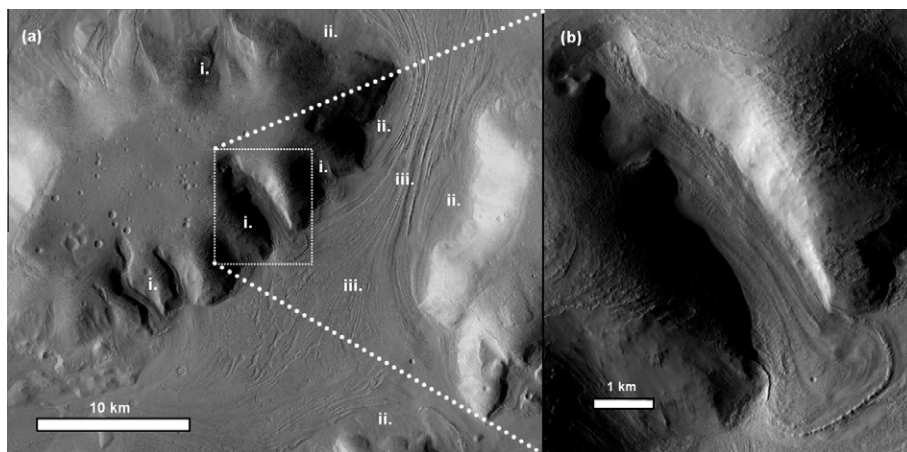


**Fig. 1.** VFFs in 'fretted terrain' (term first used by Sharp (1973)) in Protonilus Mensae – Mars' northern mid-latitudes (CTX image P22\_009455\_2214\_XN\_41N305 W). (a) The three dominant sub-classifications of VFF in context: (i) low-order glacier-like forms (GLFs); (ii) elongated rampart-like lobate debris aprons (LDAs); (iii) the distinctive, often apparently non-directional lineated valley fill (LVF). Pronounced ridges can be seen along the middle of the LVF, running parallel to the valley walls and suggesting the convergence of opposing LDA. (b) An exploded close-up of a particularly well-defined example of a GLF. Note that all images are oriented north-up and that the light source in both cases is from the left.

has a strong influence on how a glacier flows – steeper mass-change gradients generally driving faster flow. However, no firm evidence currently exists relating to the spatial expression of accumulation and ablation at the surface of martian VFFs – where atmospheric temperatures are ubiquitously and perennially below the freezing point of water. Thus, to date, no ELA has been identified on the surface of Mars.

The absence of an identifiable accumulation area on martian GLFs makes it difficult to predict or explain the distribution of these forms – which are overwhelmingly located in the mid-latitude regions of both hemispheres. Even if Mars' observed landscapes of apparently flowing ice (LVF, LDAs and GLFs) represent only the remnants of one or more larger ice masses that have since down-wasted, as some have argued (e.g. Dickson et al., 2008; Madeline et al., 2009), these deposits appear to have experienced flow in the period since a hypothesised martian glacial maximum. However, the driving forces behind this flow remain poorly understood. In particular, it is unclear whether there was (or is still) a mass-balance-type regime in operation, or whether VFFs owe their flow-like appearance only to viscous creep on sloping surfaces.

The aim of this paper is to contribute to ongoing investigations surrounding the poorly-understood mechanisms of GLF origin and evolution by (i) extending the spatial coverage and resolution of Milliken et al.'s (2003) survey and (ii) resolving a more detailed

picture (now facilitated by the availability of high-resolution, wide-angle Context Camera (CTX) data) of where and how GLFs occur in these latitudinal ranges. Specific objectives of the research are to (i) provide a high spatial resolution survey of individual GLF locations, (ii) provide an inventory of morphometric data for all individually-surveyed GLFs, and (iii) describe the spatial variation in GLF concentration and morphometry with respect to the likely controlling variables of latitude, elevation and relief. We also provide the community with an accompanying online database of location and morphometric data relating to each of the 1309 GLFs identified in this study.

## 2. Methods

### 2.1. Survey of GLF distribution

Milliken et al. (2003) previously performed a survey of 13,000 high-resolution (~1.5–6 m/pixel) MOC images. These 13,000 images yielded 146 that contained VFF-type landforms (Milliken et al., 2003). However, the narrow field of view ( $0.4^\circ$ ) of these images meant that a lower proportion of Mars' surface was observed than it is now possible to survey using recent, wider-angle ( $5.7^\circ$  field of view) imagery from the CTX mounted on the MRO

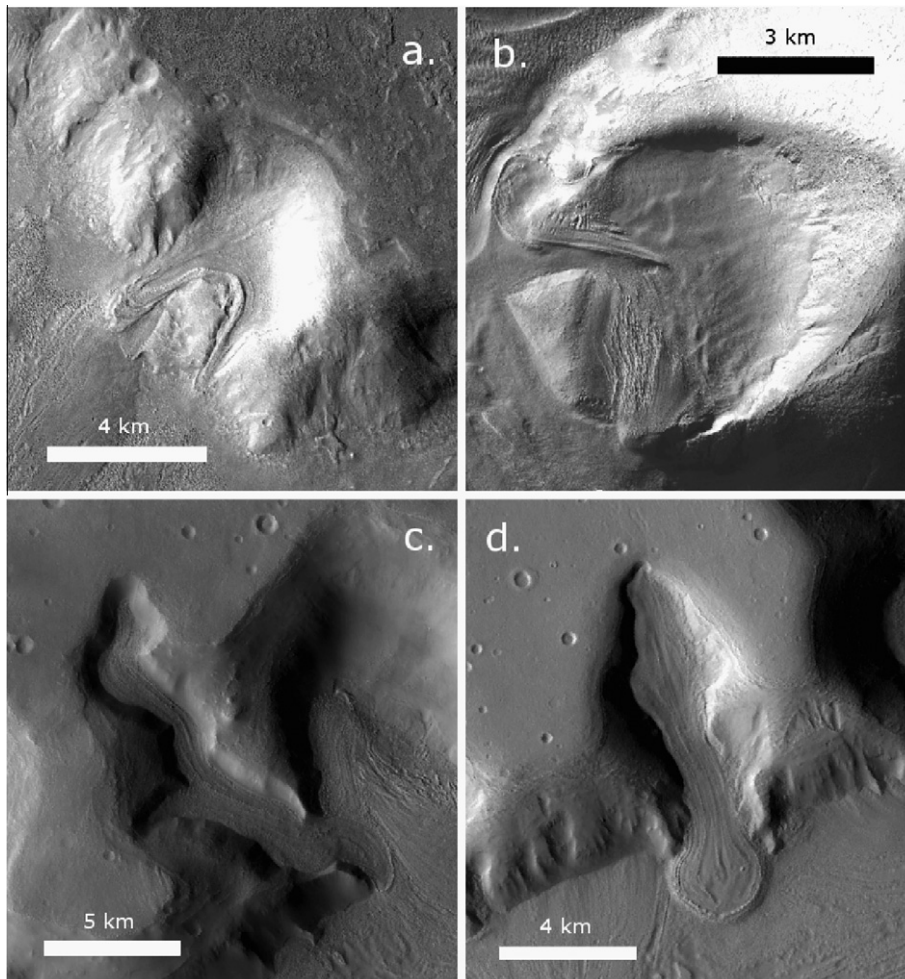


**Fig. 2.** Montage of four CTX image details showing various well-developed GLFs: (a) A double-tongued GLF situated in eastern Deuteronilus Mensae and featured in CTX image P20\_008770\_2240\_XN\_44N322W. (b) A GLF located in Eastern Hellas and featured in CTX image P02\_001727\_1391\_XN\_40S257W. (c) A convergent GLF located in Coloe Fossae and featured in CTX image P02\_001768\_2160\_XL\_36N303W. (d) A GLF which displays striking similarity to a terrestrial piedmont glacier. This example is located in Protonilus Mensae and features in CTX image P22\_009653\_2224\_XN\_42N309W. Note that in all cases images are oriented north-up and illumination is from the left (west).

spacecraft. These images are relatively high spatial resolution (6 m/pixel) and typically have a swath width of  $\sim 30$  km.

The areas lying between  $30^\circ$  and  $60^\circ$  latitude (north and south) surveyed by Milliken et al. (2003) were expanded (by  $5^\circ$  in both directions) for this survey in order to minimize the likelihood of omitting outlying GLFs that may have been missed in Milliken et al.'s (2003) survey. Thus, the regions of interest (ROI) investigated herein lie between  $25^\circ$  and  $65^\circ$  in both hemispheres. At the time of the survey, 8058 CTX images were available that had been targeted within these ROIs (Fig. 3).

## 2.2. Criteria for identifying GLFs

A set of physical criteria was devised to allow the efficient and repeatable identification of GLFs. These criteria were adapted and refined from those used by Milliken et al. (2003) to identify VFFs. Milliken identified primary and secondary lobate structures as being important indicators of flow, along with surface lineations (both parallel and transverse to the direction of movement), compressional ridges, extensional troughs, ridges at the flow front or slope base, or other general evidence of mass flow around or over obstacles. The criteria used in the survey presented here were also informed (with a view to facilitating detailed analog-based research) by the morphology and contextual characteristics of terrestrial glaciers. Thus, to be classified as a GLF in this survey, a feature was required to comply with all of the following conditions. A GLF must:

- (i) Be surrounded by topography, showing general evidence of flow over or around obstacles.
- (ii) Be distinct from the surrounding landscape, exhibiting a texture or colour different from adjacent terrains.
- (iii) Display surface foliation indicative of down-slope flow; e.g. compressional/extensional ridges, surface lineations or arcuate surface morphologies or surface crevassing.
- (iv) Have a length to width ratio  $> 1$  (i.e. be longer than it is wide), and thus be distinct from the apron-like LDA class of feature.
- (v) Have either a discernable 'head' or a discernable 'terminus' indicating a compositional boundary or process threshold.

- (vi) Appear to contain a volume of ice (or some other viscous substance), having a relatively flat 'valley fill' surface (Fig. 1b), thus differentiating it from a previously glaciated 'GLF skeleton' or assemblage of post-glacial type landforms.

A selection of well-formed GLFs is shown in Fig. 2.

## 2.3. Morphometric database

The 8058 CTX images located within the ROI (Fig. 3) were inspected by eye using the criteria listed in Section 2.2. Each image was viewed online using the 'Mars Image Explorer' interface hosted by Arizona State University ([viewer.mars.asu.edu](http://viewer.mars.asu.edu)). This facilitated efficient image inspection and GLF identification. Where GLFs were identified, JMARS ([jmars.asu.edu](http://jmars.asu.edu)) software was used to view the relevant images in a projected, georeferenced format, permitting the manual extraction of precise geographical information for each GLF. The information thus extracted included the co-ordinates (to four decimal places) of each GLF's head, terminus, true left mid-point and true right mid-point. Care was taken to avoid double counting GLFs that appeared in more than one image (i.e. repeat or stereo coverage). This was made easier by JMARS' facility for uploading and overlaying multiple CTX image stamps on a Mars geographic information system (GIS). This co-ordinate data was used to calculate the simple length and width of each GLF (as the crow flies from head to terminus or true left to true right respectively), as well as the dominant orientation (the true bearing from head to terminus of each GLF calculated using a 'great circle' function) of each individual feature. In addition, it was possible to estimate a simplified area for each GLF by multiplying its length by its mid-channel width.

## 2.4. Geographic controls

To investigate the controls responsible for observed GLF distributions, a range of environmental parameters was quantified and recorded for the immediate area surrounding each identified feature. Once this had been carried out for each GLF, it was possible to analyse the distribution of GLFs relative to variation in these potential control parameters.

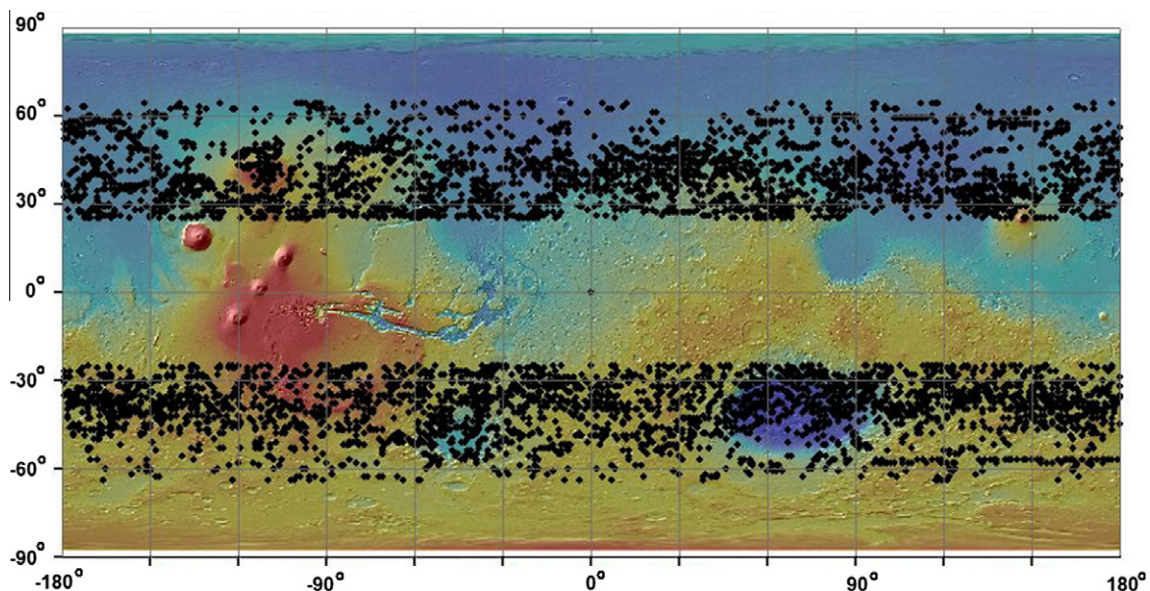


Fig. 3. Mars global map showing the locations of all 8058 CTX images used in this survey (Section 2). Positions are plotted using the central targeting co-ordinates of each image. This map gives an indication of CTX image coverage in Mars' mid-latitudes ( $25\text{--}65^\circ$  north and south) at the time of this survey.

While sampling the absolute elevation of a point on any given GLF is straightforward, extracting an approximation of local relief required a slightly more involved approach. In order to determine both characteristics for each identified GLF, data were extracted from an areal buffer of 5 km radius around the centre head of each feature. These buffer zones were scaled at 5 km on the grounds that this would provide sufficient cover to extend beyond the confines of the GLF in question (mean GLF channel width was calculated at 1.3 km), encompassing the key properties of the immediate surrounding area but without extending too far and thus skewing the data with unrelated topography. The head, rather than the centre, of each GLF was selected as the key point for this analysis as it is likely (based on the assumption that GLFs have flowed downhill from an uppermost ‘source’ area) that it is the environmental characteristics of the upper source area that are of most importance in the formation of GLFs.

Descriptive statistics for the MOLA data embedded within all pixels falling within these 5 km radius buffers were extracted for each GLF. Elevation was calculated for each GLF as a mean of its respective buffer’s collected MOLA values and relief could be approximated by calculating the standard deviation (std. dev.) of these values.

The statistics extracted in this way included (for each initial point and its surrounding buffer) the minimum elevation, the maximum elevation, the mean elevation, and the std. dev. of elevation values.

2.5. Analysis of local geographical variables

Histograms were produced describing GLF numbers as a function of the geographic variables measured both for all GLFs and for each hemisphere separately.

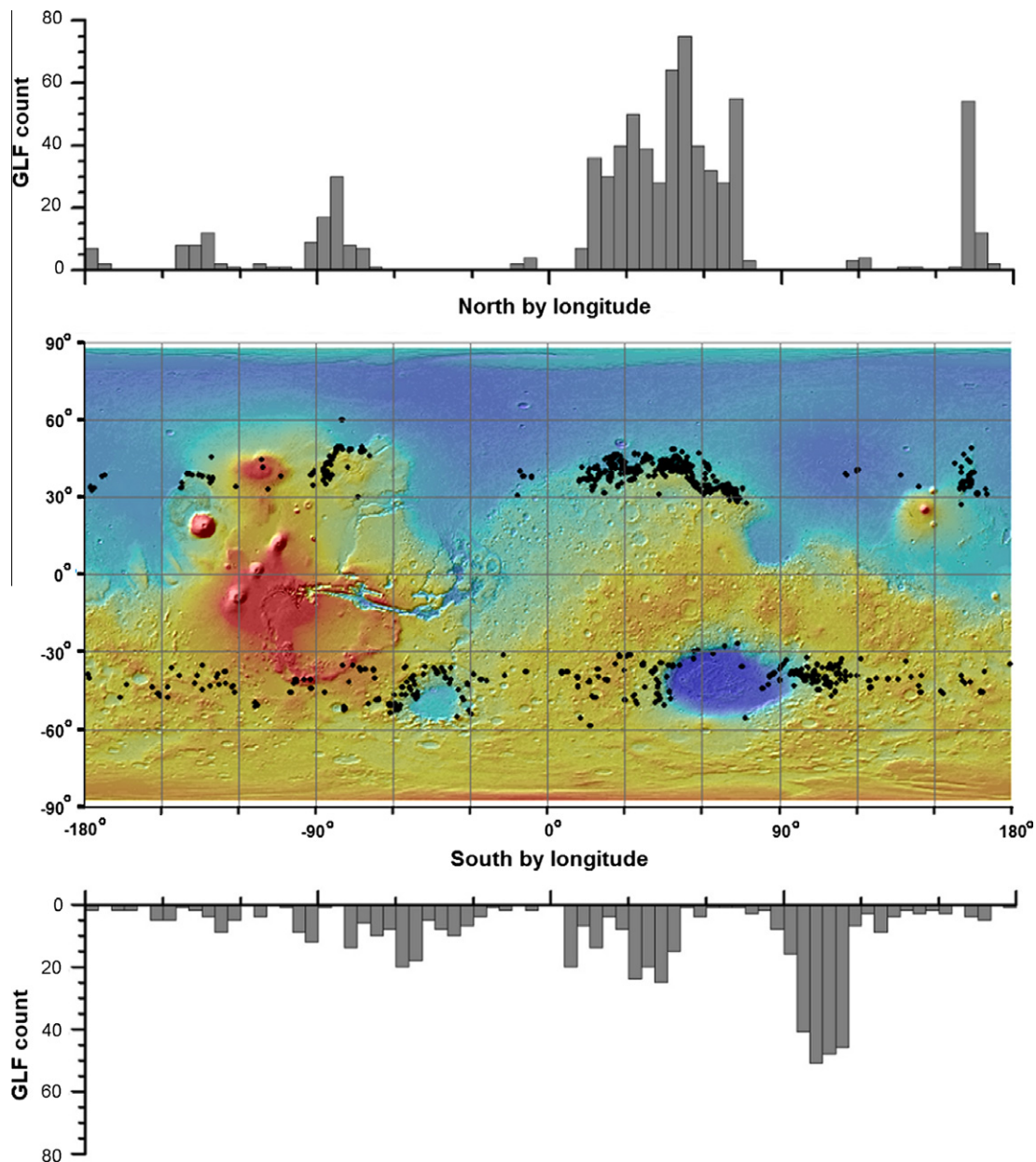


Fig. 4. Mars global map showing the mid-latitude distribution of glacier-like forms (GLFs). 1309 GLFs were identified globally. 727 were located in the northern hemisphere and 582 were located in the southern hemisphere. Histograms are displayed above and below the distribution map showing concentration of GLFs per 5° longitude. GLF locations are plotted on a MOLA hillshade projection.

ing mean, std. dev., skewness and kurtosis were then calculated for each histogram, thus quantifying the nature of the spread of GLFs relative to each geographic variable. Skewness gives an indication of the asymmetry of distributions, with negative values indicating a skew (or longer 'tail') to the left, and a positive value indicating the converse. Kurtosis provides a statistical indication of the 'peakedness' of a distribution, higher kurtosis indicating that more of the variance in a distribution is the result of infrequent, extreme deviations.

Compass rose diagrams were also plotted to illustrate GLF orientation, again on global and hemispheric scales, and equivalent angular descriptive statistics were extracted. All of these data are available from the accompanying online database.

## 2.6. Mars' mid-latitude hypsometry

MOLA data, resized to 10 pixels/degree for each hemisphere, were used to create hypsometric histograms for the study ROIs. This allowed GLF numbers, plotted by elevation, to be compared with the total surface area (corresponding to given elevational ranges) available within the ROIs.

Direct quantitative comparison was facilitated by normalising both counts (GLF and surface area) and expressing the ratio of normalised GLF count to normalised hypsometry as an index of the relative prevalence of GLFs within each elevation bin. Thus, an elevation bin containing the same fraction of all GLFs in that ROI's inventory and of the total surface area in the ROI has an elevation index of 1. If the fractional representation of GLFs is lower than that of hypsometry then the index will be  $<1$ , and conversely.

It should be noted here that the elevation data used to generate the hypsometric curves was not vetted to account for variable CTX coverage. Elevation data were included from all areas within the ROIs regardless of CTX image coverage. Some regions exist in both hemispheres where CTX coverage is sparse (for example many parts of the lowland plains north of the martian dichotomy boundary) (Fig. 3). It is therefore possible that a bias may exist where GLF population distribution is compared to ROI hypsometry.

## 3. Results

### 3.1. GLF distribution

Of the 8058 CTX images inspected, 771 (9.6%) were found to contain one or more GLFs. Of these GLF-positive images, 372 (54.3%) were located in the northern hemisphere and 399 (45.7%) were located in the southern hemisphere. In total, 1309 individual GLFs were observed, 727 (55.5%) in the northern hemisphere, and 582 (44.5%) in the southern hemisphere. The spatial distribution of these GLFs is highly clustered (Fig. 4), and particularly so in the northern hemisphere, where the often-complex highland terrain of the dichotomy boundary is intersected by the large lowland plains of Utopia Planitia, Arcadia Planitia and Acidalia Planitia (Figs. 4 and 5). High GLF concentrations are observed in areas of rough topography such as Phlegra Montes, Acheron Fossae, and the western Tempe Terra area (Figs. 4 and 5). These regions contain 56, 29 and 64 GLFs respectively, constituting 7.7%, 4.0% and 8.8% of the northern hemispheric total. However, the most densely clustered northern mid-latitude populations were observed along the dichotomy boundary in the so-called 'fretted terrains' (Sharp, 1973) of Deuteronilus Mensae, Protonilus Mensae and the Nili Fossae region located north-west of Isidis Planitia (Figs. 4 and 5). This contiguous zone featured 527 individual GLFs, constituting 72.5% of the northern hemispheric total (Fig. 4). In contrast, the lowland plains contain virtually no GLFs, although isolated examples are occasionally present within large craters (Fig. 4).

Notable GLF clustering was also observed in the southern hemisphere. High concentrations of GLFs were identified throughout the north-western rim of the Argyre Planitia impact basin ( $\sim 65$  GLFs/11.2% of the southern total), in the cratered terrains of eastern Terra Sirenum ( $\sim 35$  GLFs/6%) and in the regions east ( $\sim 186$  GLFs/32%) and west ( $\sim 60$  GLFs/10.3%) of the Hellas impact basin (Figs. 4 and 5). The most densely populated of these regions is that of eastern Hellas.

Observation of these surveyed distributions alone shows that clustered GLF populations appear to favour the middle latitudes (centred around  $\sim 40^\circ$  north and south) and areas of high relief. This is investigated further below.

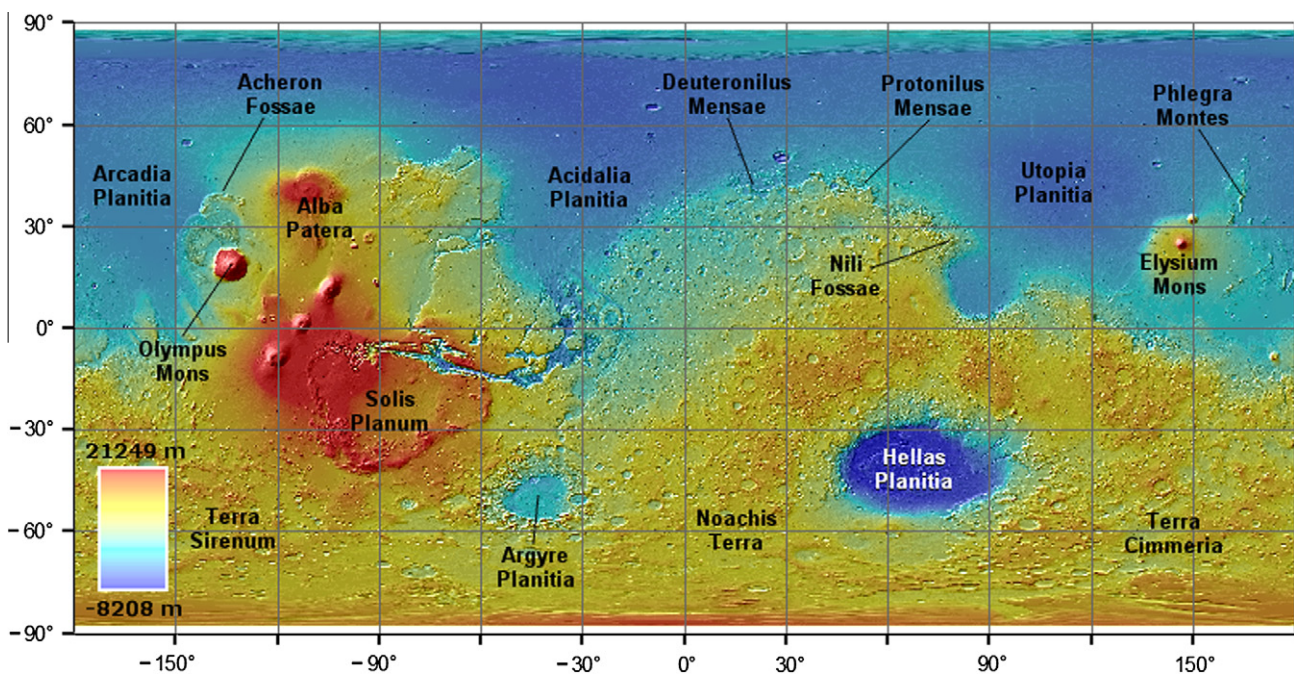


Fig. 5. A map of Mars with major landmarks and key regions annotated. Place names are marked on a MOLA digital elevation model.

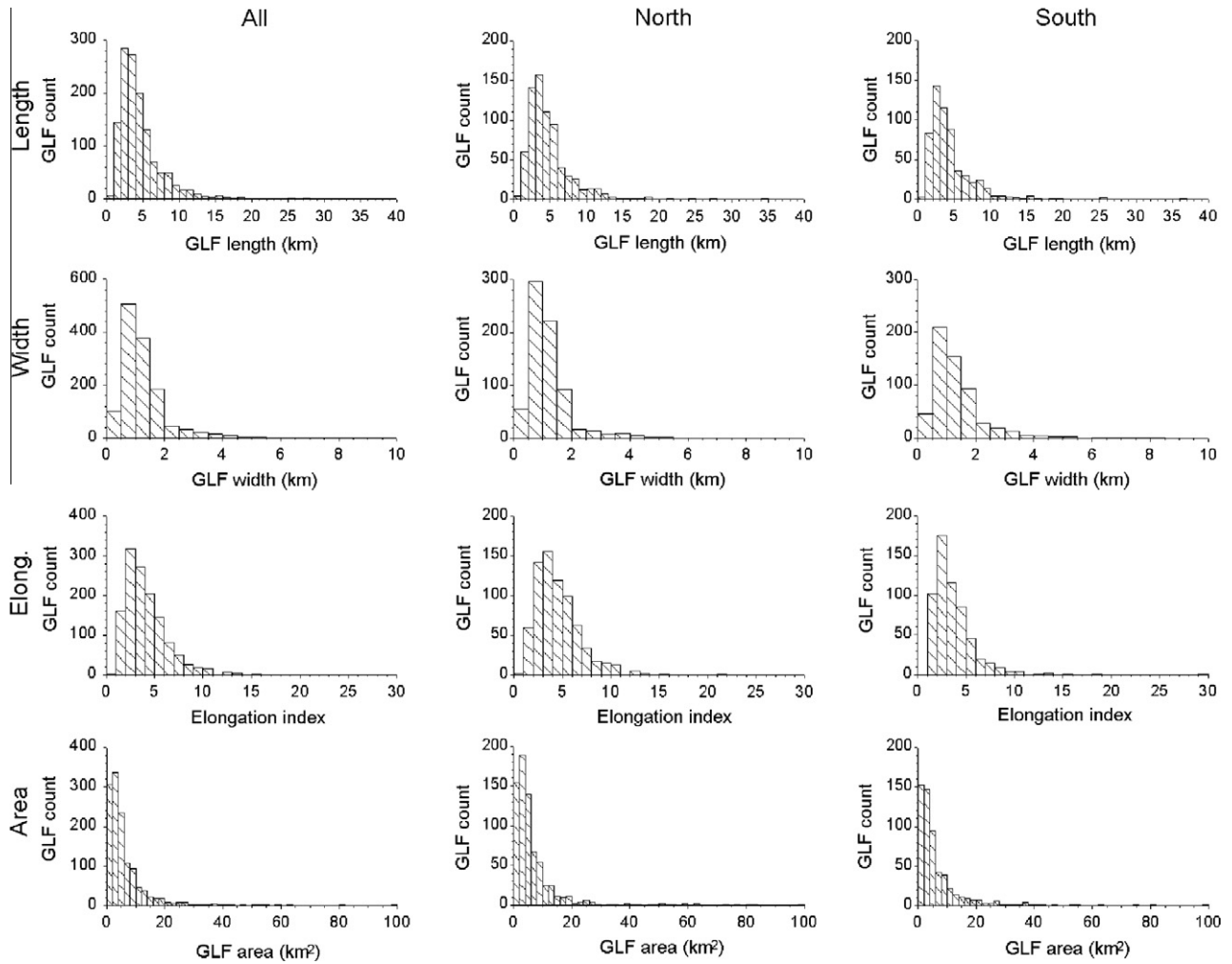


Fig. 6. Tabulated histograms showing distribution of GLF populations relative to measured length, measured width, calculated elongation (length/width) and simple area (length multiplied by width). Distributions are shown for Mars’ global GLF population and for each hemispheric population separately.

Table 1

Basic descriptive statistics of GLF morphometry, including length, width, simplified area and orientation. See also plots at Fig. 6. All values are given to within three significant figures.

ROI	GLF Char.	Mean	Std. dev.	Skewness	Kurtosis
All	Length (km)	4.66	3.37	3.29	18.4
	Width (km)	1.27	0.928	3.37	17.4
	Elongation	4.19	2.98	9.62	192
	Area (km <sup>2</sup> )	7.61	13.4	6.25	54.5
	Orientation (°)	146	117	–	–
North	Length (km)	4.91	3.42	3.14	16.3
	Width (km)	1.26	1.45	13.9	279
	Elongation	4.51	2.32	1.62	5.43
	Area (km <sup>2</sup> )	7.86	14.3	5.86	43.3
	Orientation (°)	26.6	106	–	–
South	Length (km)	4.35	3.28	3.56	22.2
	Width (km)	1.34	0.965	2.94	13.4
	Elongation	3.79	3.6	11.9	207
	Area (km <sup>2</sup> )	7.54	13.4	6.97	71
	Orientation (°)	173	73.2	–	–

Table 2

The statistical similarity (between the northern and southern hemispheres) of certain GLF properties. ‘P’ is calculated using a 2-sample ‘t’ test. Those properties and P values highlighted in bold text are found to be statistically similar at a confidence interval of 99%.

GLF property	P value
Longitude	0.000
Latitude	0.000
Length	<b>0.003</b>
Width	<b>0.274</b>
Area	<b>0.683</b>
Elongation index	0.000

statistics (mean; std. dev.; skewness and kurtosis) for each of these properties (plus orientation) are presented in Table 1. Student ‘t’ test results indicating the statistical inter-hemispheric similarity of the descriptive data shown in Table 1 are presented in Table 2. As can be seen from Table 1, overall GLF dimensions have remarkably similar mean values in both hemispheres. The ‘P’ values in Table 2 show that this similarity is statistically significant at a threshold significance of 99% for length, width and area.

### 3.2. GLF morphometry

Histograms showing GLF numbers plotted as a function of length, width, elongation (length divided by width) and area (length multiplied by width) are shown in Fig. 6. Basic descriptive

#### 3.2.1. GLF length

Mean GLF length is 4.91 km and 4.35 km in the northern and southern hemispheres respectively. The manner in which length

values vary around the mean are also similar in the two hemispheres, with the std. dev. values of 3.42 km and 3.28 km and similar values for skewness and kurtosis for the two regions (Fig. 6 and Table 1).

### 3.2.2. GLF width

In contrast to GLF length, inter-hemispheric comparison of GLF width reveals some variation. Although mean widths are statistically indistinguishable for the two hemispheres (1.26 km in the north and 1.34 km in the south), the variation in widths is greater in the north (std. dev. = 1.45 km) than in the south (std. dev. = 0.956 km). The north also displays higher skewness and kurtosis than the south (Fig. 6 and Table 1).

### 3.2.3. GLF area

GLF area (Fig. 6 and Table 1) shows broad similarities in all descriptive properties in both hemispheres.

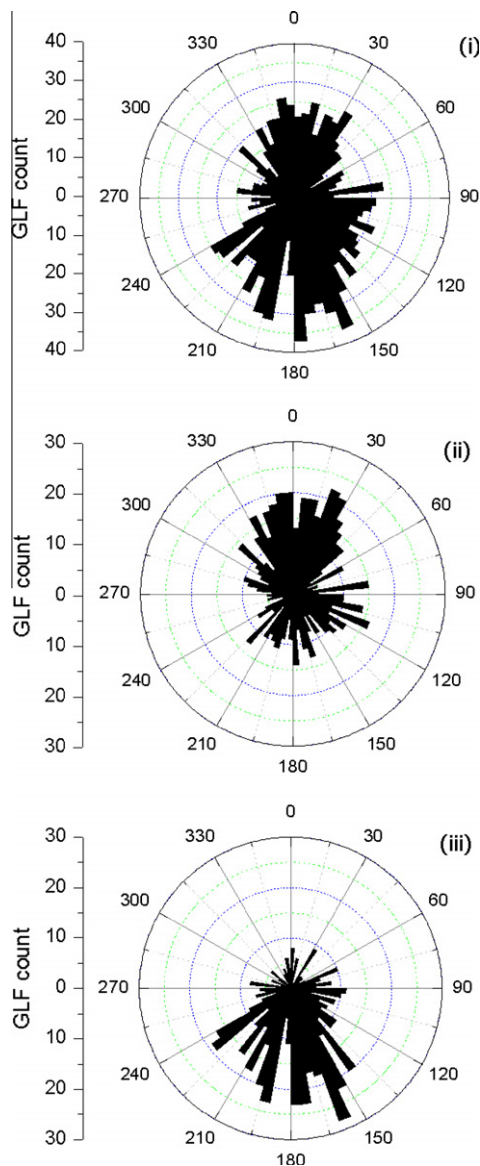


**Fig. 7.** Compass-rose diagrams showing GLF population distribution by orientation (to within 5° bins). Global population orientations are shown at (i), northern hemisphere orientations at (ii) and southern hemisphere orientations at (iii). A generalised polarisation of orientations is apparent with GLFs in both the northern and southern hemispheres tending toward a polar aspect. Interestingly, a slight easterly bias is apparent in both the northern and the southern plots.

### 3.2.4. GLF orientation

GLF orientation shows a polarised distribution (Fig. 7 and Table 1). In the northern hemisphere GLFs are predominantly orientated NNE, the mean bearing from head to terminus being 26.6°, whereas in the southern hemisphere mean orientation is south, or SSE, at 173.1° (Table 1). These results indicate a strong preference for a poleward orientation in both hemispheres, with an additional slight bias towards an easterly aspect in both hemispheres. It is also interesting to note that, although the poleward bias is a strong one in both hemispheres, the northern mid-latitudes contain a comparatively high proportion of GLFs that break with the trend and face south, whereas in the southern mid-latitudes the poleward bias is more dominant (Fig. 7). This explains the global mean's tendency to the south (146.6°) which would otherwise be surprising given the fact that the northern mid-latitudes host the larger of the two hemisphere's GLF populations. Std. dev. of orientation is, as one would expect from this observation, higher in the northern hemisphere (105.6°) than in the southern hemisphere (73.2°).

### 3.3. Local geographic parameters

As with GLF morphometry (Section 3.2), histograms of GLF population were plotted showing GLF distribution relative to the geographic parameters latitude, elevation and relief (a proxy index from the std. dev. around mean elevation; Section 2.4) (Fig. 8 and Table 3).

#### 3.3.1. Latitude

GLF distribution is similar in both hemispheres with a mean latitude of 39.3° (std. dev. = 4.9°) in the north and 40.7° (std. dev. = 5.3°) in the south. Skewness in both hemispheres (0.068 in the northern hemisphere and -0.582 in the southern hemisphere) suggests a bias towards the pole, with the 'tail' of the histogram trending towards higher latitudes in both cases (Table 3). This skew is considerably more pronounced in the south than in the north. Kurtosis is low in both hemispheres: 0.025 in the north and 0.270 in the south, describing a 'centralised' distribution in both cases.

#### 3.3.2. Elevation

Mean GLF elevations in the northern and southern hemispheres were -1366.3 m and +884.7 m respectively (relative to Mars datum) (Table 3), a difference of >2000 m. Both distributions are highly centralised with std. dev. values of only 1291.6 m in the north and 1921.9 m in the south (Fig. 8). Skewness (north and south being calculated at 0.592 and -1.283 respectively) and kurtosis (calculated as 2.374 and 3.887) values for both hemispheres are also relatively low (Table 3). So, in both hemispheres GLF distribution shows a marked preference for (and strong centralisation around) a certain range of elevations, although this range differs considerably in each hemisphere.

Considering GLF distribution in relation to the hypsometry of the ROIs yields an apparent contrast between the two hemispheres (Fig. 9). Fig. 9i indicates that the hypsometry of the two hemisphere's ROIs are markedly different, with land surface in the northern hemisphere clustering around an elevation of ~-4000 m and land surface in the southern hemisphere clustering around an elevation of ~(+)2000 m. However, comparison of the equivalent GLF elevation histograms with these hypsometric distributions (Fig. 9ii) reveals that, while the distributions of both GLF and land surface coincide in the southern hemisphere, they do not in the north. Here, GLFs are strongly shifted towards higher elevations, occurring predominantly in the range -3000 to -500 m (whereas the modal land surface elevation range oc-

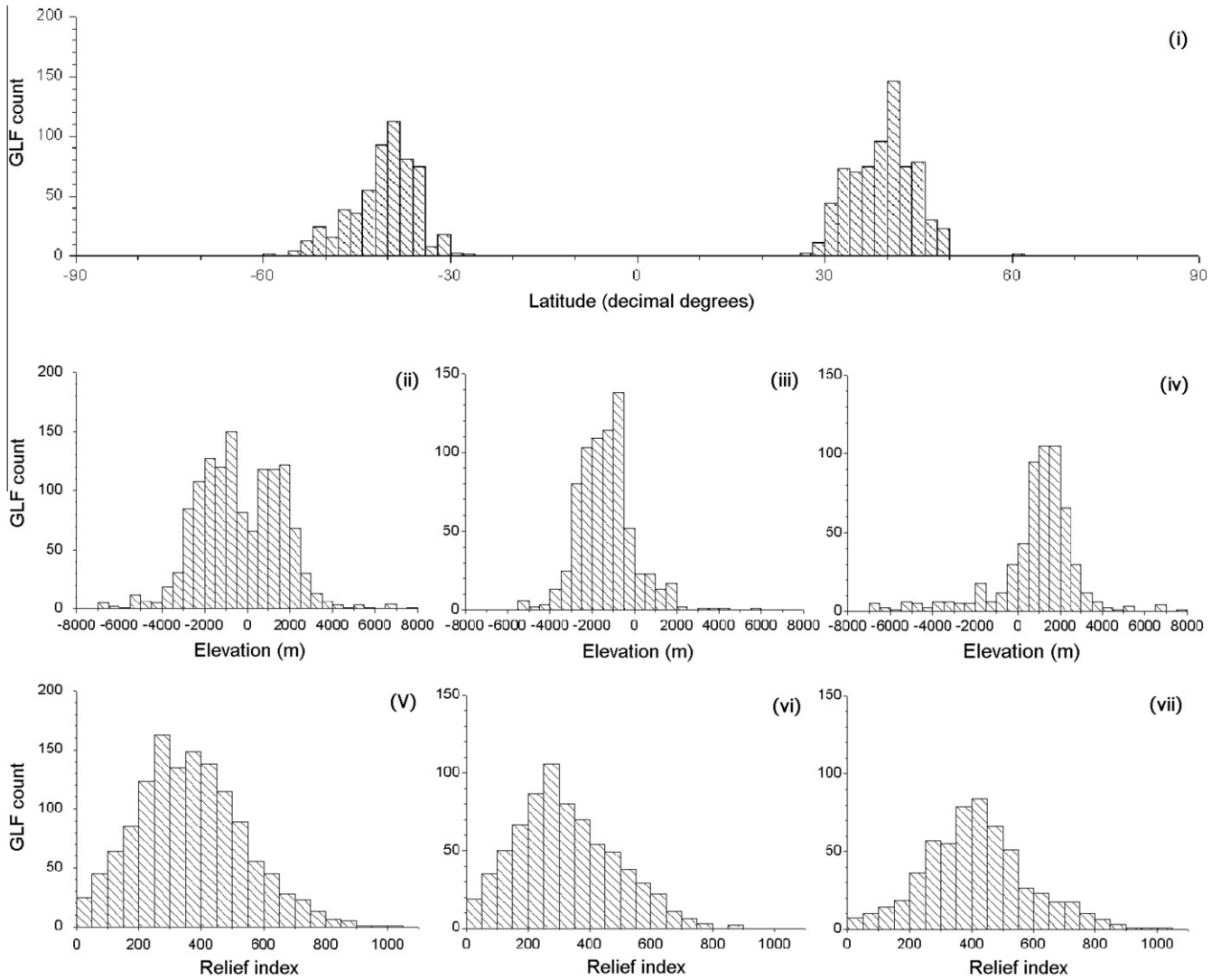


**Fig. 8.** Histograms showing distribution of GLF population relative to global latitude (i) (in 2° bins); global elevation (ii); northern hemispheric elevation (iii); southern hemispheric elevation (iv); global relief (v); northern hemispheric relief (vi); and southern hemispheric relief (vii).

**Table 3**

Basic descriptive statistics of GLF distribution relative to latitude, elevation and relief (std. dev. of local elevation values). See also histograms at Fig. 8. All values are given to within 3 significant figures.

ROI	Parameter	Mean	Std. dev.	Skewness	Kurtosis
All	Latitude (°)	–	–	–	–
	Elevation (m)	–366	1954	0.049	0.387
	Relief (m)	364	171	0.413	0.108
North	Latitude (°)	39.3	4.94	0.0682	0.0249
	Elevation (m)	–1366	1292	0.592	2.37
	Relief (m)	323	161	0.489	–0.074
South	Latitude (°)	–40.7	5.27	–0.582	0.270
	Elevation (m)	885	1922	–1.28	3.89
	Relief (m)	417	168	0.347	0.447

curs at –4500 to –3500 m). This effect is clearly illustrated by a plot of the ratio of the normalised GLF data to the normalised surface-area data against elevation (Fig. 9iii). While this ratio remains fairly close to 1 across most elevation bands in the southern hemisphere, it deviates in the northern hemisphere towards large positive values in the elevation range –2000 to 0 m (peaking at a value of 7 in the –1000 to –500 m bin).

3.3.3. Relief

The GLF relief index has a mean value of 323 (std. dev. = 161) in the northern hemisphere and 417 (std. dev. = 168) in the southern hemisphere (Table 3). This suggests that GLFs occur in areas of optimum (i.e. neither maximum or minimum) relief in both hemispheres, although both are slightly different (with the higher of the two being in the southern hemisphere). The southern hemispheric population also shows a more Gaussian peaked distribution with a kurtosis of 0.447 compared to the northern hemisphere population’s kurtosis of –0.074. The northern population also has a slightly larger skewness of 0.489 compared to 0.374 in the south.

4. Interpretation of results

4.1. GLF morphometry

The striking similarity of GLF morphometries in the northern and the southern hemispheres (Table 1 and Fig. 6) suggests that all GLFs share a common composition and that they form and evolve in a similar fashion. Mean length, width and area are statistically similar at a confidence interval of 99% in both hemispheres despite topography being highly variable. The main difference ap-

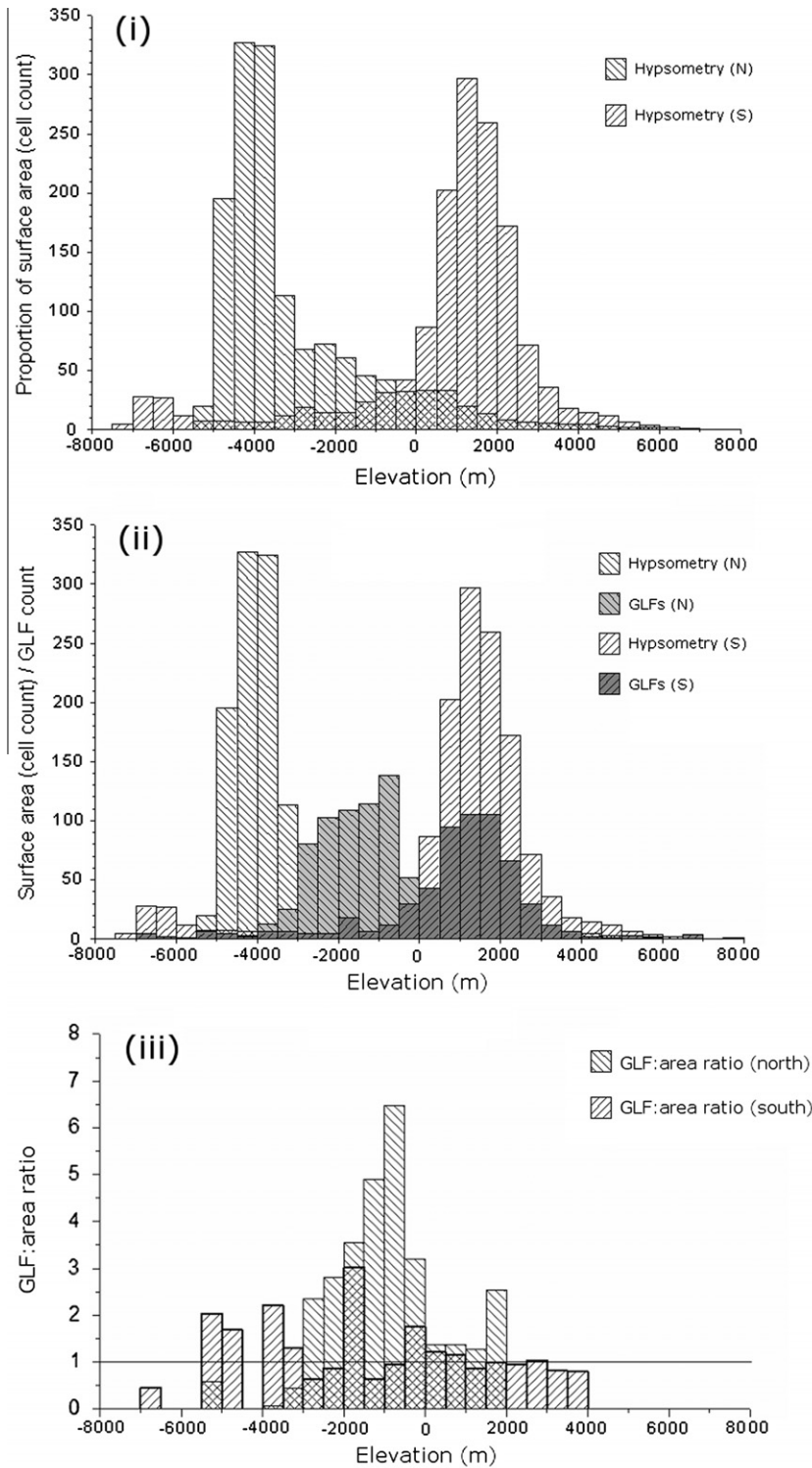


**Fig. 9.** (i) Hypsometric curves for the surveyed ROIs (25–65° north and south). Both plots (overlaid) are based on MOLA data, re-scaled to a resolution of 10 pixels/degree, and show the proportion of the land surface in each ROI to fall within set 500 m elevation bins. (ii) Comparison of GLF distribution by elevation to the hypsometric curves of both mid-latitude ROIs. As can be seen, the bimodal nature of both data series shows similarities. GLF distribution relative to elevation is split, with the northern GLF population trending toward the lower elevations that are heavily represented in the northern mid-latitude hypsometric curve. (iii) A comparison of GLF:area ratio (area as a proportion of ROI hypsometry) in the northern and southern hemispheres. A value of '1' in each column represents a GLF population proportional to the percentage of surface area characterised by a given elevational range. Values >1 represent elevational ranges where GLFs are over-represented, while values of <1 denote elevational ranges where GLFs are under-represented. As can be seen from the overlaid plots – the GLF population in the southern hemisphere is distributed relatively proportionately relative to elevation by area. In the northern hemisphere however, GLFs are under-represented at elevations <–3000 m (elevation relative to Mars datum), and heavily over-represented at elevations between –3000 m and 0 m.

pears to be that GLF width is (slightly) more variable in the northern ROI than in the south: with std. dev., skewness and kurtosis all

being higher in the northern than in the southern hemisphere. As the mean values are still broadly similar – and the distributions

visible in Fig. 6 closely resemble each other – this does not give grounds to infer that a fundamentally different process is in operation. Rather, perhaps, the nature of the underlying terrain exercises some control, for example the tendency of GLFs in the southern hemisphere to occur in craters compared to the butte and mesa landscape of the northern hemisphere's fretted terrains (for example Fig. 1).

Regarding orientation, the pronounced preference for a poleward aspect for the majority of GLFs in both hemispheres (Fig. 7) is consistent with observations made in previous studies of VFFs within craters at a more local scale (Berman et al., 2009). However, this study reveals the global dominance of this pattern, indicating that it is highly unlikely that the observed trend results from localised factors. This preference for a poleward aspect is similar to glacier emplacement on Earth where persistent ice accumulation and survival are more likely in pole-facing alcoves where insolation is lower (e.g. Unwin, 1972). This correspondence between Earth and Mars supports the interpretation of GLFs, and by extension associated VFFs, as being glacier-like in nature. It also lends credence to arguments that GLFs grow and flow under a similar regime (sensitive to processes of accumulation and ablation and the balance between the two) to that of their terrestrial counterparts. However, it is important to note that this does not necessarily imply that the modes of accumulation and ablation that operate on Earth and Mars are at all similar. Current GLF distributions on Mars reflect not only where ice accumulated, but also where it has survived in the face of a changing planetary climate. Therefore, patterns of current GLF orientation cannot be used as evidence of any orientational preference in initial mass emplacement or, by extension, any specific mode of ice precipitation.

An interesting feature of the observed pattern of GLF orientations is the bias in both hemispheres toward an easterly aspect (Fig. 7 and Table 1). In the northern hemisphere, mean GLF orientation is 26.6°, while in the south the mean is 173.1°. Conway et al. (2011) revealed a similar eastward bias in the orientation of gullies situated in the walls of craters in Terra Cimmeria and Noachis Terra. The authors attributed these gullies to de-stabilisation of the mid-latitude icy mantle terrain, indicating a possible link to GLFs and other VFFs as was also suggested by Milliken et al. (2003) for VFFs and gullies and by Christensen (2003) for 'snowpacks' and gullies. These studies suggest that liquid water may have incised the gullies as ice or snow deposits melted at some point during Mars' recent geological history. However, no explanations have yet been presented for the apparent eastward bias in either gully orientation or VFF orientation.

## 4.2. GLF population relative to local geographic parameters

### 4.2.1. Latitude

The distribution of GLFs relative to latitude shows a strong clustering of hemispheric populations around ~40° latitude (39.3° in the northern hemisphere and -40.7° in the southern hemisphere) (Fig. 7 and Table 2). These population clusters correspond very closely to each other and the std. dev. of population around these values is low, indicating that latitude exerts a very strong control on GLF population.

Interestingly, both populations, although highly clustered by latitude, do exhibit statistical skewness towards the pole, with GLF population in both cases falling more gradually towards higher latitudes than towards the equator. This is not as apparent in the north, where there is a gap in GLF population between 50° and 60° latitude (Fig. 8i), but outlying GLFs in craters at latitudes between 60° and 63° north suggest that environmental conditions are still suitable for GLF formation, implying a non-climatic control in this 'empty zone'. We interpret this hiatus in terms of the dichotomy boundary, which has effectively 'cropped' GLF popula-

tion, elevation and relief north of the boundary being so low as to have suppressed GLF formation (or potentially inhibited GLF preservation). It is therefore tempting to suggest that if regional topography were not split in such a fashion then a skew such as that visible in the south would also be seen here.

GLF population may increase with distance from the pole as the icy mantling deposit described by Kreslavsky and Head (2000, 2002) gradually de-stabilises with increasing proximity to the equator (Conway et al., 2011). The mean or 'optimal' latitudes of 39.3° and -40.7° (in the north and south respectively) could then represent effective thresholds whereby climate has de-stabilised ground ice to the point where it flows most readily, departure from this threshold latitude in a poleward direction leading to increased stability of the mantling material, while equatorward proximity induces more rapid ice de-stabilisation and ablation.

The evidence would appear to suggest that the dependence of GLF distribution upon latitude is to a large extent the result of conditions and factors in play during initial GLF formation. GLF concentration manifestly increases with distance from the poles (up until an observed threshold as discussed above), which represents a break from the terrestrial norm, which sees the abundance of glacial ice generally decreasing in tandem with latitude. Terrestrial analogy suggests that on Mars too, which has a broadly similar climatic regime if not entirely similar conditions, ice should be less likely to survive at lower latitudes. As the converse is (to an extent) true, we propose that the signal in these results originates predominantly in GLF formation and to a lesser extent in GLF preservation.

### 4.2.2. Elevation

The highly clustered distribution of GLFs relative to elevation in both hemispheres (Fig. 8) suggests a preference for certain altitudinal ranges, indicating that as well as latitude, elevation exerts an important control over where and how GLFs form (or where GLFs have survived). However, GLFs are clustered around different altitudinal ranges in the two hemispheres (Fig. 9ii).

Inspection of the plot showing GLF population as a normalised proportion of hypsometry (Fig. 9iii) shows that in the southern ROI, where GLF population relative to elevation corresponds comparatively well to hypsometry (and elevations are almost ubiquitously in excess of -3000 m), GLFs are quite evenly represented (proportionally) relative to the available land surface within each elevational band. In the northern ROI, however, GLFs are under-represented in elevational bands below ~-3000 m, and markedly over-represented in those lying between -3000 m and 0 m (Mars datum). One possible explanation for the observed pattern in both hemispheres is that a threshold elevation exists, below which GLF formation does not occur, or at least GLF formation is strongly suppressed (some outlying examples have been mapped in lower-lying areas such as in craters north of the martian dichotomy boundary and in the Hellas basin). Our evidence reveals that this threshold lies at ~-3000 m.

These observations contribute to the case for martian GLFs having been sensitive to a mass balance regime that is in some ways similar to that which exists on Earth; elevation-related factors apparently exerting an important influence on the emplacement and (possibly) the flow of ice.

It must be clearly stated in this case that the pattern of GLF distribution pertaining to elevation could very possibly be due to variable GLF preservation rather than initial formation. GLFs may have existed above and below the observed elevation thresholds but have subsequently ablated or been otherwise destroyed. However, despite this uncertainty, the sensitivity of GLF distribution to elevation seems clear and the ~-3000 m threshold seems key.

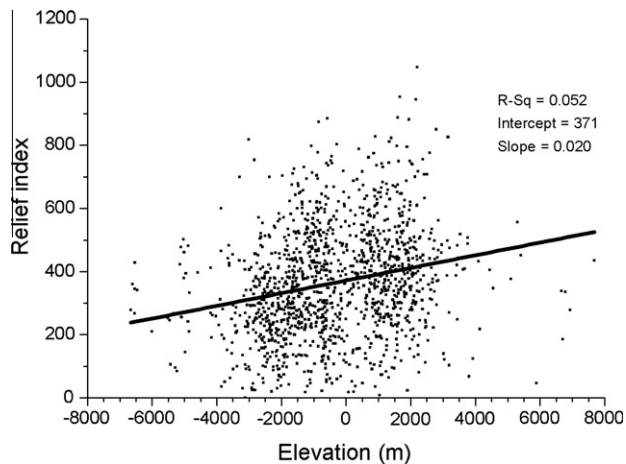


**Fig. 10.** A scatter plot showing the relationship between elevation and relief on an individual GLF basis. The Pearson's 'R', intercept and slope of the regression (plotted as a line) are all marked on the graph, showing a very weak correlation. This infers that elevation and relief, on a localised scale, are very weakly related, reducing the risk of co-linearity when GLF distribution relative to each independent variable is investigated.

#### 4.2.3. Relief

The distribution of GLF populations relative to relief shows a preference for mid-range values and strong clustering about the mean in both hemispheres. However, skewness in both hemispheric population distributions indicate that GLFs are preferentially located in 'moderately' rough topography. A higher mean in the southern ROI (417 units in the south compared to 323 units in the north) indicates that GLFs occupy rougher terrain in the south. This may be due to the preponderance of GLFs that are situated on crater walls in the south. In the north, the heads of many GLFs are situated at or near the top of a cliff or at the edge of a raised plateau. Southern GLFs often originate part-way up crater rims, the incline of the basin extending farther above the upper reaches of the GLF in question. Thus the immediate area adjacent to the GLF's head would have a higher relief than were it to coincide with the edge of a plateau.

These distributions imply that a link exists between GLF distribution and relief: GLFs favouring moderate relief areas and neither flat nor precipitous terrain. Since relief does not correlate with elevation (Fig. 10) any relationship between GLF distribution and relief is real and not a by-product of elevation. This suggests that GLFs are produced by gravity-induced creep, the propensity of accumulated ice to flow being a function of local slope.

This hypothesis necessitates the existence of an upper and lower relief threshold beyond which GLF-type flow does not occur. This is easy to imagine for low-relief areas where channelized, gravity-induced flow is unlikely under associated extremely low shear stresses. It is more difficult to explain for high-relief surfaces. In such areas perhaps icy material has simply weathered away through sublimation enhanced by exposure, or has broken away in the fashion of rock-fall debris, gradients being too high to permit gradual, viscous flow. This hypothesis dovetails once again into the issue of GLF formation opposed to GLF preservation and would benefit from further research.

## 5. Conclusions

Visual analysis of 8058 CTX images revealed the presence of 1309 GLFs on the surface of Mars. Analyses performed on the distribution of these GLFs indicate that they have developed through the interplay of various factors.

GLFs mapped across Mars' mid-latitudes share broadly similar morphometries suggesting a common composition and evolutionary history (Fig. 6 and Table 1). At the largest scale, latitude appears to exert the strongest, 'first order' control over GLF distribution. Their strong preference for certain latitudes, and the statistical skewness of these populations toward the poles, coupled with the predominantly poleward orientation of most individual GLFs on a global scale, strongly suggests a sensitivity to climate and insolation, as previously proposed on the basis of local and regional studies. At a local scale, the siting of GLFs appears to be closely controlled by elevation. Thus elevation may be considered to exert a 'second-order' control, with the optimal elevation around which GLFs cluster in each hemisphere (GLFs show a strong preference for a tight range in both ROIs) varying between the north and the south. However, inspection of each ROI's hypsometry and the distribution of GLFs relative to the spread of available elevations suggests that on a planetary scale GLFs occur most readily above an altitude of  $\sim$ 3000 m. This suggests that ice only accumulates (or has merely only survived) above this elevation, indicating that quasi-mass-balance conditions either are, or perhaps were, in operation.

The fact that the highest density of GLFs occurs in the middle elevations and GLFs are not statistically over-represented at the highest (Fig. 9) contrasts the terrestrial scenario. This may be due to Mars' exceptionally broad hypsometry and the characteristics of Mars' atmospheric stratigraphy.

Finally, relief appears to play an important, perhaps 'third-order' control that is independent of elevation, GLFs occurring predominantly in areas of moderate relief.

The extent to which present-day GLF distribution has been affected by processes of ice removal and preservation since a hypothesised last glacial event is difficult to ascertain, particularly given the gaps in current understanding of GLF composition. Terrestrial glaciers exhibit great variety in their debris content and/or their surface debris load, and this variable debris component can have a profound effect on ablation rates and thus long-term ice survival (e.g. Nakawo and Young, 1981; Benn and Evans, 1998, p. 72; Hindmarsh et al., 1998). Equivalent diversity in material properties almost certainly exists on Mars. It may be, therefore, that GLF preservation and thus present-day distribution is also partly affected by composition. Little direct information is available on GLF composition, and although the morphometric analyses performed during this research indicate some degree of uniformity, further research aimed at improving our understanding of this issue could be of great value. A detailed inspection of the landscapes in the vicinity of and immediately adjacent to current GLFs could be of particular benefit, perhaps yielding evidence of mass deposition and thus former ice-borne debris loads, as well as perhaps expanded extents of former GLFs which could enhance our understanding of where and how ice has survived and where it has not.

We suggest that GLFs presently occur where icy material, preferentially distributed within well-defined latitudinal and elevational ranges, has undergone local, gravity-induced flow and deformation in response to local relief. It could well be that adjacent areas of similar elevation and latitude, but of lower relief, house substantial ice reservoirs, but such deposits have not (yet) undergone flow and thus are not apparent as GLFs. Indeed, the widespread presence in these latitude bands of texturally distinct surface 'mantle' terrains believed to represent ice-dust mixtures (Mustard et al., 2001; Milliken et al., 2003; Head et al., 2003) suggests this is likely the case.

Martian GLFs therefore may not exhibit accumulation areas or ablation areas as exist on Earth, except perhaps where they flow downhill sufficiently to cross an elevational threshold which may lie at  $\sim$ 3000 m, beyond which the survival of any single GLF will be compromised by climatic factors.

## Acknowledgments

We thank the California Institute of Technology and NASA JPL for the time and facilities that were placed at our disposal during the early stages of this research. Also, acknowledgement is due to the National Environmental Research Council (NERC) who funded the primary author of this research.

## Appendix A. Supplementary data

Supplementary data associated with this article can be found, in the online version, at doi:10.1016/j.icarus.2011.10.020.

## References

- Arfstrom, J., Hartmann, W.K., 2005. Martian flow features, moraine-like ridges, and gullies: Terrestrial analogs and interrelationships. *Icarus* 174, 321–335.
- Baker, D.M.H., Head, J.W., Marchant, D.R., 2010. Flow patterns of lobate debris aprons and lineated valley fill north of Ismeniae Fossae, Mars: Evidence for extensive mid-latitude glaciation in the Late Amazonian. *Icarus* 207, 186–209.
- Benn, D.I., Evans, D.J.A., 1998. *Glaciers and Glaciation*. Arnold, London.
- Berman, D.C., Crown, D.A., Bleamaster, L.F., 2009. Degradation of mid-latitude craters on Mars. *Icarus* 200, 77–95.
- Christensen, P.R., 2003. Formation of recent martian gullies through melting of extensive water-rich snow deposits. *Nature* 422, 45–48.
- Conway, S.J., Mangold, N., Ansan, V., 2011. Crater Shape Evolution with Latitude in Terra Cimmeria, Mars – Implications for Climate. LPSC XLII, Houston, TX.
- Dickson, J.L., Head, J.W., Marchant, D.R., 2008. Late Amazonian glaciation at the dichotomy boundary on Mars: Evidence for glacial thickness maxima and multiple glacial phases. *Geology* 36, 411–414.
- Fanale, F.P., Salvail, J.R., Zent, A.P., Postawko, S.E., 1986. Global distribution and migration of subsurface ice on Mars. *Icarus* 67, 1–18.
- Forget, F., Haberle, R.M., Montmessin, F., Levrard, B., Head, J.W., 2006. Formation of glaciers on Mars by atmospheric precipitation at high obliquity. *Science* 311, 368–371.
- Head, J.W., Mustard, J.F., Kreslavsky, M.A., Milliken, R.E., Marchant, D.R., 2003. Recent ice ages on Mars. *Nature* 426, 797–802.
- Head, J.W. et al., 2005. Tropical to mid-latitude snow and ice accumulation, flow and glaciation on Mars. *Nature* 434, 346–351.
- Head, J.W., Marchant, D.R., Dickson, J.L., Kress, A.M., Baker, D.M., 2010. Northern mid-latitude glaciation in the Late Amazonian period of Mars: Criteria for the recognition of debris-covered glacier and valley glacier landform deposits. *Earth Planet. Sci. Lett.* 294, 306–320.
- Hindmarsh, R.C.A., Van Der Wateren, F.M., Verbers, A.L.L.M., 1998. Sublimation of ice through sediment in Beacon Valley, Antarctica. *Geogr. Ann.* 80, 209–219.
- Holt, J.W. et al., 2008. Radar sounding evidence for buried glaciers in the southern mid-latitudes of Mars. *Science* 322, 1235–1238.
- Hubbard, B., Milliken, R.E., Kargel, J.S., Limaye, A., Souness, C., 2011. Geomorphological characterization and interpretation of a mid-latitude glacier-like form: Hellas Planitia, Mars. *Icarus* 211, 330–346.
- Kargel, J.S., 2004. *Mars: A Warmer, Wetter Planet*. Springer Praxis Books.
- Kreslavsky, M.A., Head, J.W., 2000. Kilometer-scale roughness of Mars' surface: Results from MOLA data analysis. *J. Geophys. Res.* 100, 11781–11799.
- Kreslavsky, M.A., Head, J.W., 2002. Mars: Nature and evolution of young latitude-dependent water-ice-rich mantle. *Geophys. Res. Lett.* 29 (15). doi:10.1029/2002GL015392.
- Li, H., Robinson, M.S., Jurdy, D.M., 2005. Origin of martian northern hemisphere mid-latitude lobate debris aprons. *Icarus* 176 (2), 382–394.
- Madeleine, J.B., Forget, F., Head, J.W., Levrard, B., Montmessin, F., Millour, E., 2009. Amazonian northern mid-latitude glaciation on Mars: A proposed climate scenario. *Icarus* 203, 390–405.
- Marchant, D.R., Head, J.W., 2003. Tounge-shaped lobes on Mars: Morphology, nomenclature, and relation to rock glacier deposits. In: *Sixth International Conference on Mars*. 3091.pdf.
- Milliken, R.E., Mustard, J.F., Goldsby, D.L., 2003. Viscous flow features on the surface of Mars: Observations from high-resolution Mars Orbiter Camera (MOC) images. *J. Geophys. Res.* 108 (E6), 5057.
- Morgan, G.A., Head, J.W., Marchant, D.R., 2009. Lineated valley fill (LVF) and lobate debris aprons (LDA) in the Deuteronilus Mensae northern dichotomy boundary region, Mars: Constraints on the extent, age and episodicity of Amazonian glacial events. *Icarus* 202, 22–38.
- Mustard, J.F., Cooper, C.D., Rifkin, M.K., 2001. Evidence for recent climate change on Mars from the identification of youthful near-surface ground ice. *Nature* 412, 411–414.
- Nakawo, M., Young, G.J., 1981. Field experiments to determine the effect of a debris layer on ablation of glacier ice. *Ann. Glaciol.* 2, 85–91.
- Pelletier, J.D., Comeau, D., Kargel, J., 2009. Controls of glacial valley spacing on Earth and Mars. *Geomorphology*. doi:10.1016/j.geomorph.2009.10.018.
- Plaut, J.J., Safaeinili, A., Holt, J.W., Phillips, R.J., Head, J.W., Sue, R., Putzig, N.E., Frigeri, A., 2009. Radar evidence for ice in lobate debris aprons in the mid-northern latitudes of Mars. *Geophys. Res. Lett.* 36, L02203.
- Schon, S.C., Head, J.W., Milliken, R.E., 2009. A recent ice age on Mars: Evidence for climate oscillations from regional layering in mid-latitude mantling deposits. *Geophys. Res. Lett.* 36, L15202. doi:10.1029/2009GL038554.
- Sharp, R.P., 1973. Mars: Fretted and chaotic terrains. *J. Geophys. Res.* 78 (20), 4073–4083.
- Squyres, S.W., Carr, M.H., 1986. Geomorphic evidence for the distribution of ground ice on Mars. *Science* 213, 249–253. doi:10.1126/science.231.4735.249.
- Sugden, D.E., John, B.S., 1990. *Glaciers and Landscape*. Arnold Publishing.
- Touma, J., Wisdom, J., 1993. The chaotic obliquity of Mars. *Science* 259, 1294–1297.
- Unwin, D.J., 1972. The distribution and orientation of corries in northern Snowdonia, Wales. *Trans. Inst. British Geograph.* 58, 85–97.